

Simultaneous synthesis and consolidation of nanostructured MgAl_2O_4 - $\text{Mg}_3\text{Al}_4\text{Ti}_3\text{O}_{25}$ composite by pulsed current activated sintering and its mechanical properties

In-Jin Shon^{a,*}, Jung-Mann Doh^b, Jin-Kook Yoon^b and Song-Lee Du^a

^aDivision of Advanced Materials Engineering and the Research Center of Advanced Materials Development, Engineering College, Chonbuk National University 561-756, Korea

^bAdvanced Functional Materials Research Center, Korea Institute of Science and Technology, PO Box 131, Cheongryang, Seoul 130-650, Korea

Nanopowders of Al_2O_3 , TiO_2 and MgO were fabricated by high energy ball milling. The simultaneous synthesis and sintering of nanostructured MgAl_2O_4 - $\text{Mg}_3\text{Al}_4\text{Ti}_3\text{O}_{25}$ composite was investigated by the pulsed current activated sintering process. The advantage of this process is that it allows very quick densification to near theoretical density and inhibition of grain growth. A highly dense nanostructured MgAl_2O_4 - $\text{Mg}_3\text{Al}_4\text{Ti}_3\text{O}_{25}$ composite was produced with the simultaneous application of 80 MPa pressure and a pulsed current of 2000A within one minute. The grain sizes and mechanical properties of MgAl_2O_4 - $\text{Mg}_3\text{Al}_4\text{Ti}_3\text{O}_{25}$ composite sintered at 1150 °C were investigated.

Key words: Sintering, Composite, Nanostructured material, Powder metallurgy.

Introduction

The attractive properties of MgAl_2O_4 is high hardness of (16 GPa), low density (3.58 g/cm^3), high melting point (2135 °C), high chemical inertness and high thermal shock resistance [1-3]. Because of its excellent properties, MgAl_2O_4 ceramic has been employed mainly in the glass and steel industries, etc. However, as in the case of many ceramic materials, the current concern about these materials focuses on their low fracture toughness below the ductile-brittle transition temperature [4]. To improve their mechanical properties, the approach commonly utilized has been the addition of a second phase to form composites and to make nanostructured materials.

Nanocrystalline materials have received much attention as advanced engineering materials with improved physical and mechanical properties [5, 6]. As nano materials possess high strength, high hardness, excellent ductility and toughness, undoubtedly, more attention has been paid to the application of nano materials [7, 8]. In recent days, nanocrystalline powders have been developed by the thermochemical and thermomechanical process named as the spray con-version process (SCP), co-precipitation and high energy milling [9-11]. The sintering temperature of high energy mechanically milled powder is lower than that of unmilled powder due to the increased reactivity, internal and surface energies, and surface area

of the milled powder, which contribute to its so-called mechanical activation [12-14]. However, the grain size in sintered materials becomes much larger than that in pre-sintered powders due to a rapid grain growth during a conventional sintering process. Therefore, even though the initial particle size is less than 100 nm, the grain size increases rapidly up to 2 μm or larger during conventional sintering [15]. So, controlling grain growth during sintering is one of the keys to the commercial success of nanostructured materials. In this regard, the pulsed current activated sintering method (PCASM) which can make dense materials within 2 minutes has been shown to be effective in achieving this goal [16-18].

In this study, we investigated the simultaneous synthesis and sintering of MgAl_2O_4 - $\text{Mg}_3\text{Al}_4\text{Ti}_3\text{O}_{25}$ composite by the PCAS method. The goal of this research is to produce dense nanostructured MgAl_2O_4 - $\text{Mg}_3\text{Al}_4\text{Ti}_3\text{O}_{25}$ composite. In addition, we also studied the microstructure and mechanical properties of MgAl_2O_4 - $\text{Mg}_3\text{Al}_4\text{Ti}_3\text{O}_{25}$ composite.

Experimental Procedure

The MgO powder with a grain size of $< 45 \mu\text{m}$ and 99.8% purity and Al_2O_3 powder with a grain size of $< 3 \mu\text{m}$ and 99.99% purity and TiO_2 powder with a grain size of $< 45 \mu\text{m}$ and 99.8% purity used in this research was supplied by Alfa. The powders (40 mole.% MgO -30 mole.% Al_2O_3 -30 mole.% TiO_2) were first milled in a high-energy ball mill (Pulverisette-5 planetary mill) at 250 rpm for 10 hrs. Tungsten carbide balls (9 mm in diameter) were used in a sealed cylindrical

*Corresponding author:
Tel : +82 63 270 2381
Fax: +82 63 270 2386
E-mail: ijshon@chonbuk.ac.kr

stainless steel vial under an argon atmosphere. The grain sizes of the MgO , TiO_2 and Al_2O_3 were calculated from the full width at half-maximum (FWHM) of the diffraction peak by Suryanarayana and Grant Norton's formula [19]:

$$B_r(B_{\text{crystalline}} + B_{\text{strain}}) \cos\theta = k \lambda / L + \eta \sin\theta \quad (1)$$

where B_r is the full width at half-maximum (FWHM) of the diffraction peak after instrumental correction; $B_{\text{crystalline}}$ and B_{strain} are the FWHM caused by a small grain size and internal stress, respectively; k is a constant (with a value of 0.9); λ is the wavelength of the X-ray radiation; L and η are the grain size and internal strain, respectively; and θ is the Bragg angle. The parameters B and B_r follow Cauchy's form with the relationship: $B = B_r + B_s$, where B and B_s are the FWHM of the broadened Bragg peaks and the standard sample's Bragg peaks, respectively.

The powders were placed in a graphite die (outside diameter, 35 mm; inside diameter, 10 mm; height, 40 mm) and then introduced into the pulsed current activated sintering (PCAS) apparatus shown schematically in Fig. 1. The PCAS apparatus includes a 30 kW power supply which provides a pulsed current (on time; 20 μ sec, off time; 10 μ sec) through the sample, and a 50 kN uniaxial load. The system was first evacuated and a uniaxial pressure of 80 MPa was applied. A pulsed current was then activated and maintained until the densification rate was negligible, as indicated by the real-time output of the shrinkage of the sample. The shrinkage was measured by a linear gauge measuring the vertical displacement. Temperatures were measured by a pyrometer focused on the surface of the graphite die. At the end of the process, the pulsed current was turned off and the sample cooled to room temperature. The process was carried out under a vacuum of 5.33 Pa.

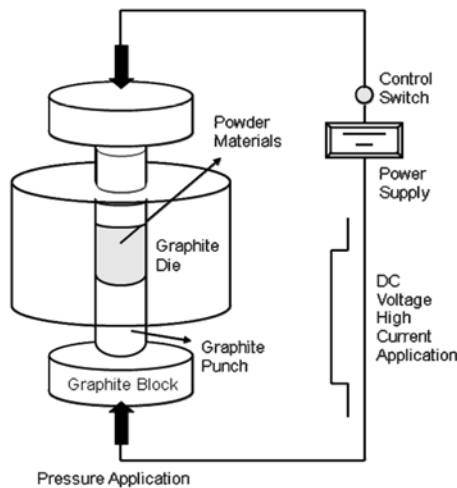


Fig. 1. Schematic diagram of apparatus for pulsed current activated sintering.

Microstructural information was obtained from product samples, which had been polished and etched using thermal etching for 1 hr at 1050 °C. Compositional and microstructural analyses of the products were made through X-ray diffraction (XRD), and a field emission scanning electron microscope (FE-SEM) with energy dispersive X-ray spectrometer (EDS). Vickers hardness was measured by performing indentations at a load of 5 kg and a dwell time of 15 sec.

Results and Discussion

Fig. 2 shows X-ray diffraction patterns of the MgO , TiO_2 and Al_2O_3 powders after high-energy ball milling for 10h. Only MgO , TiO_2 and Al_2O_3 peaks are detected and $MgAl_2O_4$ and $Mg_3Al_4Ti_3O_{25}$ peaks are not detected. So, synthesis does not occur during the ball milling. Fig. 3 shows a plot of $B_r \cos\theta$ versus $\sin\theta$ of MgO , TiO_2 and Al_2O_3 milled for 10 hrs to calculate the particle size from XRD data. The average grain sizes of the milled MgO , TiO_2 and Al_2O_3 powders determined by Suryanarayana and Grant Norton's formula were about 10, 64 and 41 nm, respectively.

FE-SEM images of MgO , TiO_2 and Al_2O_3 powders after milling for 10 hrs are shown in Fig. 4. MgO and Al_2O_3 powders have a round shape, refinement with milling and some agglomeration. In EDS, Al, Si, Mg, and O peaks are detected and heavier contaminants, such as W and Fe from a ball or milling container, were not detected. The variations of the shrinkage displacement and temperature with the heating time for pulsed 2000A during the sintering of the high energy ball milled MgO , TiO_2 and Al_2O_3 powders under a pressure of 80 MPa are shown in Fig. 5. The application of the pulsed current resulted in shrinkage due to consolidation. As the pulsed current was applied, thermal expansion showed. And then the shrinkage abruptly increased at about 850 °C. Fig. 6

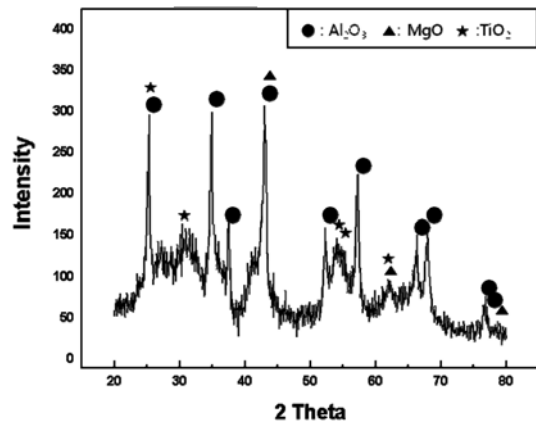


Fig. 2. X-ray diffraction patterns of the TiO_2 , Al_2O_3 and MgO powders milled for 10 hrs. Fig. 3. Plot of $B_r (B_{\text{crystalline}} + B_{\text{strain}}) \cos\theta$ versus $\sin\theta$ for (a) Al_2O_3 , (b) MgO and (c) TiO_2 powder milled for 10 hrs.

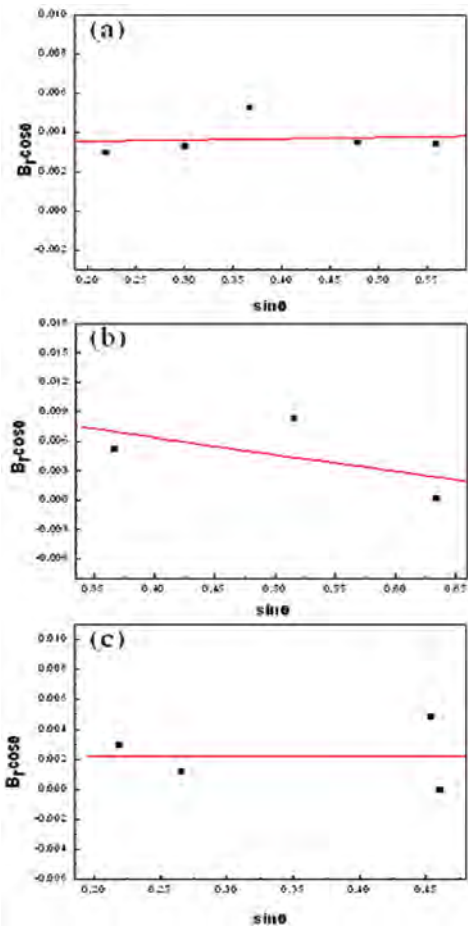


Fig. 3. Plot of $B_r (B_{\text{crystalline}} + B_{\text{strain}}) \cos\theta$ versus $\sin\theta$ for (a) Al_2O_3 , (b) MgO and (c) TiO_2 powder milled for 10 hrs.

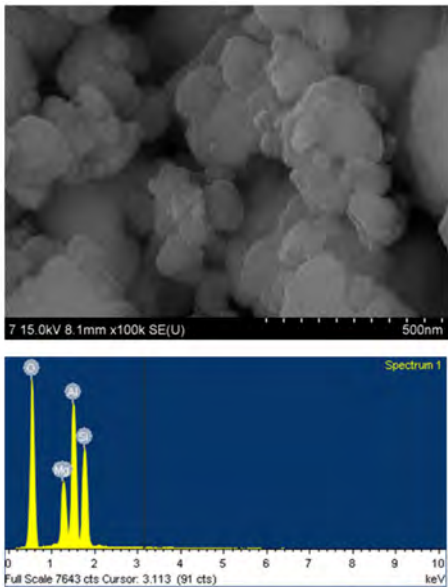


Fig. 4. FE-SEM image of the TiO_2 , Al_2O_3 and MgO powders milled for 10 hrs.

shows the XRD pattern of a specimen sintered at 1150°C from the high energy ball milled MgO , TiO_2 and Al_2O_3 powders. In Fig. 6, MgAl_2O_4 and $\text{Mg}_3\text{Al}_4\text{Ti}_3\text{O}_{25}$

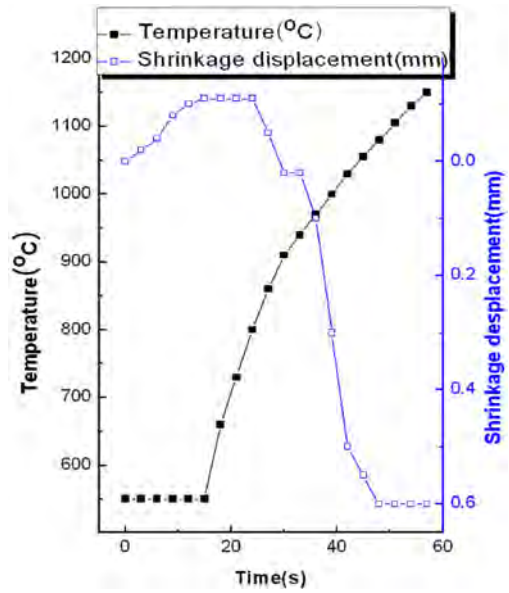


Fig. 5. Variations of temperature and shrinkage with heating time during the sintering of TiO_2 , Al_2O_3 and MgO powders milled for 10 hrs.

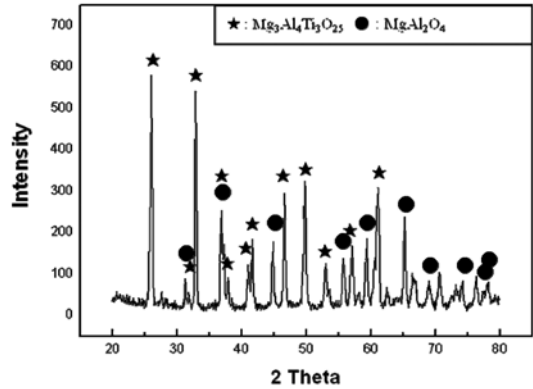


Fig. 6. XRD pattern of specimen of sintered MgAl_2O_4 - $\text{Mg}_3\text{Al}_4\text{Ti}_3\text{O}_{25}$ composite from the high energy ball milled TiO_2 , MgO and Al_2O_3 powders.

peaks are detected. From the X-ray diffraction, the interaction between these phases, i.e.,



is thermodynamically feasible.

Fig. 7 shows plot of $B_r \cos\theta$ versus $\sin\theta$ for MgAl_2O_4 and $\text{Mg}_3\text{Al}_4\text{Ti}_3\text{O}_{25}$ in Suryanarayana and Grant Norton's formula [19]. The average grain size of the MgAl_2O_4 and $\text{Mg}_3\text{Al}_4\text{Ti}_3\text{O}_{25}$ calculated from the XRD data using Suryanarayana and Grant Norton's formula was about 20 and 65 nm. Thus, the average grain size of the sintered MgAl_2O_4 and $\text{Mg}_3\text{Al}_4\text{Ti}_3\text{O}_{25}$ is not greatly larger than that of the initial powders, indicating the absence of substantial grain growth during sintering. This retention of the grain size is attributed to the high heating rate and the relatively short term exposure of the powders to the high tem-

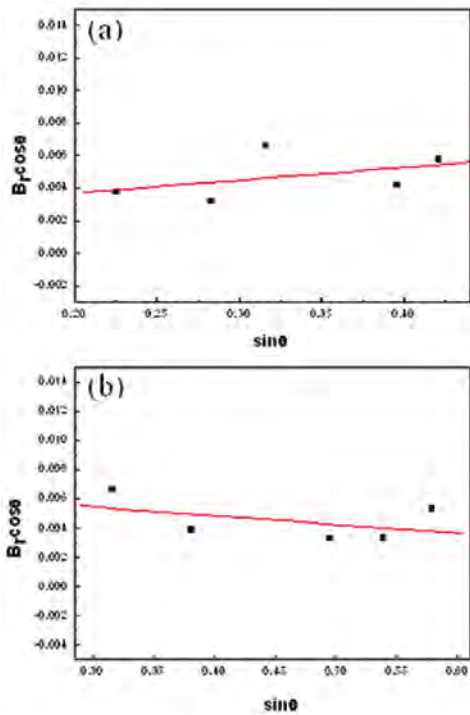


Fig. 7. Plot of B_r ($B_{crystalline} + B_{strain}$) $\cos\theta$ versus $\sin\theta$ for $MgAl_2O_4$ and $Mg_3Al_4Ti_3O_{25}$ in composite sintered from the TiO_2 , Al_2O_3 and MgO powders milled for 10 hrs.

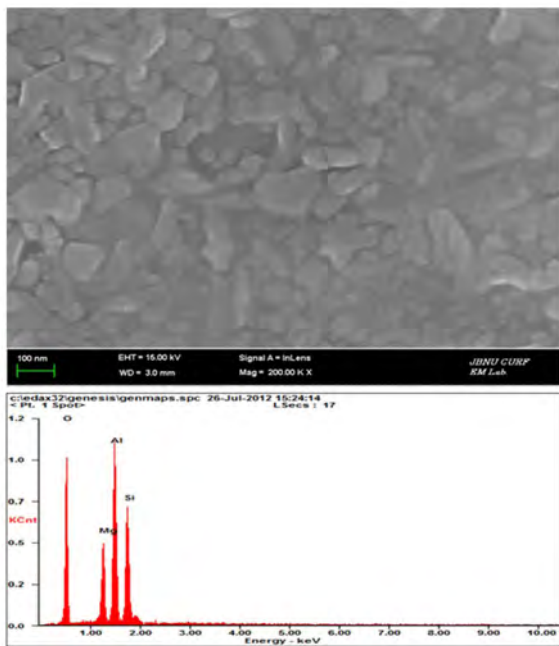


Fig. 8. FE-SEM image of sintered $MgAl_2O_4$ - $Mg_3Al_4Ti_3O_{25}$ composite.

perature. FE-SEM images of $MgAl_2O_4$ - $Mg_3Al_4Ti_3O_{25}$ composite sintered from MgO , TiO_2 and Al_2O_3 powders milled for 10h are shown in fig. 8. The $MgAl_2O_4$ and $Mg_3Al_4Ti_3O_{25}$ consists of nanocrystallines.

The role of the current (resistive or inductive) in sintering and or synthesis has been the focus of several attempts aimed at providing an explanation of the

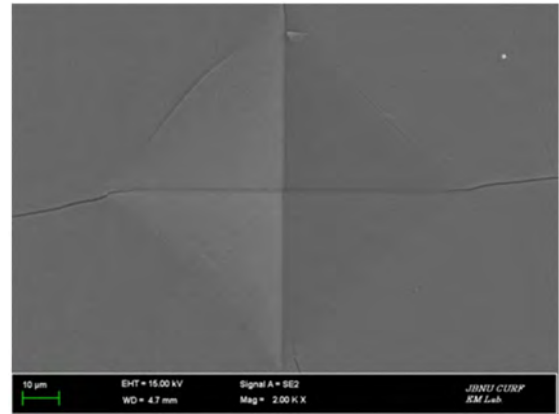


Fig. 9. Vickers indentation in the $MgAl_2O_4$ - $Mg_3Al_4Ti_3O_{25}$ composite sintered from milled $3TiO_2$ - $4MgO$ - $3Al_2O_3$ powders.

observed enhancement of sintering and the improved characteristics of the products. The role played by the current has been variously interpreted, the effect being explained in terms of a rapid heating rate due to Joule heating, the presence of a plasma in the pores separating powder particles, and the intrinsic contribution of the current to mass transport [20-23].

Vickers hardness measurements were performed on polished sections of the $MgAl_2O_4$ - $Mg_3Al_4Ti_3O_{25}$ composite using a 5 kg load and 15 sec dwell time. The Vickers hardness of $MgAl_2O_4$ - $Mg_3Al_4Ti_3O_{25}$ composite sintered from Al_2O_3 , TiO_2 and MgO powders milled for 10 hrs was 710 kg/mm^2 .

Indentations with large enough loads produced median cracks around the indent. Fig. 9 shows Vickers indentations in the $MgAl_2O_4$ - $Mg_3Al_4Ti_3O_{25}$ composite sintered from TiO_2 - MgO - Al_2O_3 powders. One to three additional cracks were observed to propagate from the indentation corners. The length of these cracks permits an estimation of the fracture toughness of the materials by means of the expression [24]:

$$K_{IC} = 0.204(c/a)^{-3/2} \cdot H_v \cdot a^{1/2} \quad (3)$$

where c is the trace length of the crack measured from the center of the indentation, a is one half of the average length of the two indent diagonals, and H_v is the hardness. The calculated fracture toughness value for the $MgAl_2O_4$ - $Mg_3Al_4Ti_3O_{25}$ composite sintered from TiO_2 - Al_2O_3 - MgO powders is about $3 \text{ MPam}^{1/2}$. As in the case of the hardness value, the toughness value is the average of five measurements. The fracture toughness of $MgAl_2O_4$ - $Mg_3Al_4Ti_3O_{25}$ composite is higher than that of monoclinic $MgAl_2O_4$.

Summary

Nanopowders of TiO_2 , Al_2O_3 and MgO were fabricated by high energy ball milling. Using the rapid sintering method, PCAS, the densification of nanostructured

MgAl₂O₄-Mg₃Al₄Ti₃O₂₅ composite was accomplished within one minute from mechanically activated powders using high energy ball milling. The average grain size of the MgAl₂O₄ and Mg₃Al₄Ti₃O₂₅ were about 20 and 65 nm. The Vickers hardness and fracture toughness of MgAl₂O₄-Mg₃Al₄Ti₃O₂₅ composite sintered from TiO₂, Al₂O₃ and MgO powders milled for 10 hrs were 710 kg/mm² and 3 MPa · m^{1/2}, respectively. The fracture toughness of MgAl₂O₄-Mg₃Al₄Ti₃O₂₅ composite is higher than that of monoclinic MgAl₂O₄.

Acknowledgments

This work is partially supported by KIST Future Resource Research Program and this work was supported by the Human Resources Development program (No. 20134030200330) of the Korea Institute of Energy Technology Evaluation and Planning (KETEP) grant funded by the Korea government Ministry of Trade, Industry and Energy.

References

1. S. Anappan, L.J. Berchmans, C.O. Augustin, *Mater. Lett.* 58 (2004) 2283-2289.
2. C. Baudin, R. Martinez, P. Pena, *J. Am. Ceram. Soc.* 78 [7] (1995) 1857-1862.
3. P. Hing, *J. Mater. Sci.* 11 (1976) 1919-1926.
4. In-Jin Shon, In-Yong Ko, Hyun-Su Kang, Kyung-Tae Hong, Jung-Mann Doh, and Jin-Kook Yoon, *Met. Mater. Int.*, Vol. 18, No. 1 (2012) 109-113.
5. M.S. El-Eskandarany, *J. Alloys & Compounds.* 305 (2000) 225-38.
6. L. Fu, L.H. Cao, Y.S. Fan, *Scripta Materialia.* 44 (2001) 1061-68.
7. K. Niihara, A. Niihara, *Advanced structural Inorganic Composite*, Elsevier Scientific Publishing Co., Trieste, Italy (1990).
8. S. Berger, R. Porat, R. Rosen, *Progress in Materials.* 42 (1997) 311-20.
9. Z. Fang, J.W. Eason, *Int. J. of Refractory Met. & Hard Mater.* 13 (1995) 297-303.
10. A.I.Y. Tok, L.H. Luo, F.Y.C. Boey, *Materials Science and Engineering A* 383 (2004) 229-234.
11. Wonbaek Kim, Hee-Ji Wang, Ki-Min Roh, Sung-Wook Cho, Jae-Won Lim, and In-Jin Shon, *Korean J. Met. Mater.* 50 (2012) 310-315.
12. F. Charlot, E. Gaffet, B. Zeghmati, F. Bernard, J. C. Liepce, *Mater. Sci. Eng. A* 262 (1999) 279-285.
13. I.J. Shon, B.R. Kim, J.M. Doh, J.K. Yoon, K.D. Woo, *Journal of Alloys and Compounds.* 489 (2010) L4-L8.
14. M.K. Beyer, H. Clausen-Schaumann, *Chem. Rev.* 105 (2005) 2921-2926.
15. J. Jung, S. Kang, *Scripta Materialia.* 56 (2007) 561-564.
16. Song-Lee Du, In-Jin Shon, Jung-Mann Doh, Bang-Ju Park, and Jin-Kook Yoon, *Korean J. Met. Mater.* 50 (2012) 449-454.
17. In-Yong Ko, Na-Ra Park, and In-Jin Shon, *Korean J. Met. Mater.* Vol. 50, No. 5 (2012) 369-374.
18. N.R. Park, I.Y. Ko, J.M. Doh, J.K. Yoon, I.J. Shon, *Journal of Ceramic Processing Research.* 12 (2011) 660-663.
19. C. Suryanarayana, M.G. Norton, *X-ray Diffraction A Practical Approach*, Plenum Press, New York (1998).
20. Z. Shen, M. Johnsson, Z. Zhao and M. Nygren, *J. Am. Ceram. Soc.* 85 (2002) 1921-27.
21. J.E. Garay, U. Anselmi-Tamburini, Z.A. Munir, S.C. Glade and P. Asoka-Kumar, *Appl. Phys. Lett.* 85 (2004) 573-575.
22. J.R. Friedman, J.E. Garay, U. Anselmi-Tamburini and Z.A. Munir, *Intermetallics.* 12 (2004) 589-597.
23. J.E. Garay, J.E. Garay, U. Anselmi-Tamburini and Z.A. Munir, *Acta Mater.* 51 (2003) 4487-95.
24. K. Niihara, R. Morena, and D.P.H. Hasselman, *J. Mater. Sci. Lett.* 1 (1982) 12-16.